Journal of Modern Optics
Publication details, including instructions for authors and subscription information:
http://www.tandfonline.com/loi/tmop20

Passively mode-locked fiber laser sensor for acoustic pressure sensing

Shun Wang[a], Ping Lu[a], Hao Liao[a], Liang Zhang[a], Deming Liu[a] & Jiangshan Zhang[b]
[a] School of Optical and Electronic Information, National Engineering Laboratory for Next Generation Internet Access System, Huazhong University of Science and Technology, Wuhan 430074, China
[b] Department of Electronics and Information Engineering, Huazhong University of Science and Technology, Wuhan 430074, China
Published online: 15 Jan 2014.

To cite this article: Shun Wang, Ping Lu, Hao Liao, Liang Zhang, Deming Liu & Jiangshan Zhang (2013) Passively mode-locked fiber laser sensor for acoustic pressure sensing, Journal of Modern Optics, 60:21, 1892-1897, DOI: 10.1080/09500340.2013.865801

To link to this article: http://dx.doi.org/10.1080/09500340.2013.865801

Journal of Modern Optics, 2013
Vol. 60, No. 21, 1892–1897, http://dx.doi.org/10.1080/09500340.2013.865801

Passively mode-locked fiber laser sensor for acoustic pressure sensing

Shun Wang[a], Ping Lu[a]*, Hao Liao[a], Liang Zhang[a], Deming Liu[a] and Jiangshan Zhang[b]

[a]*School of Optical and Electronic Information, National Engineering Laboratory for Next Generation Internet Access System, Huazhong University of Science and Technology, Wuhan 430074, China;* [b]*Department of Electronics and Information Engineering, Huazhong University of Science and Technology, Wuhan 430074, China*

(*Received 3 June 2013; accepted 8 November 2013*)

The development is reported of a multi-longitudinal mode fiber laser sensor based on passive mode locking employing carbon nanotubes in the laser cavity. A polymer membrane is employed beneath the pre-strained erbium-doped fiber (EDF) to convert the sound pressure disturbance into axial strain, alter the cavity length, and induce a shift of the longitudinal modes beat. Hence, acoustic pressure measurement can be carried out by detecting the shift of the beat frequency. Experimental results show comparable strain and sound pressure sensitivity of ~0.5 kHz/με and 147.2 Hz/Pa, respectively. The proposed sensor is an alternative for the measurement of acoustic pressure and possesses the advantages of good stability and ease of interrogation.

Keywords: fiber laser sensor; passive mode locking; multi-longitudinal mode; acoustic pressure sensor

1. Introduction

In recent years, interest in fiber optic acoustic sensors has increased owing to their many important applications, such as the fiber optic hydrophones [1], ultrasonic sensors for structural health monitoring or industrial process monitoring [2,3], and acoustic vibration detection in seismological observation and localization [4]. The fiber optic acoustic pressure sensor is one type of fiber optic acoustic sensor and most of these sensors are of the interferometric type, especially the Fabry–Perot arrangement [5–7], which achieves much higher sensitivities than conventional piezoelectric counterparts. However, phase error caused by machine and environmental interference is a severe problem for this type of sound pressure sensor. To solve this problem, fiber laser sensors are thought to be good candidates for acoustic pressure measurement as a result of their demodulation in the frequency domain. Owing to their ultra-high sensitivity to temperature and strain as well as multiplexed ability, both distributed feedback (DFB) and distributed Bragg reflector (DBR) types have been investigated for environmental disturbances sensing [8,9]. In comparison with the DFB laser sensor, it is easier and cheaper to fabricate a DBR one. However, the poor stability induced by mode hopping and spatial-hole burning would prove problematic for a common DBR multi-longitudinal mode laser sensor, so frequency stabilization measurements are necessary. The passive mode-locking technique, which employs carbon nanotubes (CNTs), is a widely used method for mode locking and frequency stabilization [10].

In this paper, a passively mode-locked fiber laser sensor (FLS) is reported and experimental results described for strain and acoustic pressure measurement. We obtained results for strain sensitivity ~0.5 kHz/με and acoustic pressure sensitivity 147.2 Hz/Pa, which are comparable with the reported related values [11,12]. In addition, the proposed sensor shows advantages of good stability for its mode-locked application and simplicity of interrogation in the frequency domain. It could be a good candidate for applications in acoustic field measurement.

2. Principle

When a round polymer membrane works as a transducer which transforms the acoustic pressure disturbance into its deformation, it stretches the pre-strained erbium-doped fibre (EDF) and finally causes additional strain. Consequently, this induced strain will cause a corresponding linear beat frequencies shift.

The schematic configuration of a passively mode-locked FLS based on the multi-longitudinal mode is shown in Figure 1. A simple and low-cost linear laser cavity is formed by an optical fiber coupler (OC1) and a broadband optical reflector. Outputs 3 and 4 of OC1 are spliced together, so an equivalent broadband grating is formed with optical power of output 1, i.e. $P_1 = P_2(1 - 2K)^2$ when we inject optical power in port 2. The splitting ratios of OC1 and OC2 are 54:46 and 50:50, respectively. A section of EDF about 3 m long is inserted into the linear cavity to supply enough gain for

*Corresponding author. Email: pluriver@mail.hust.edu.cn

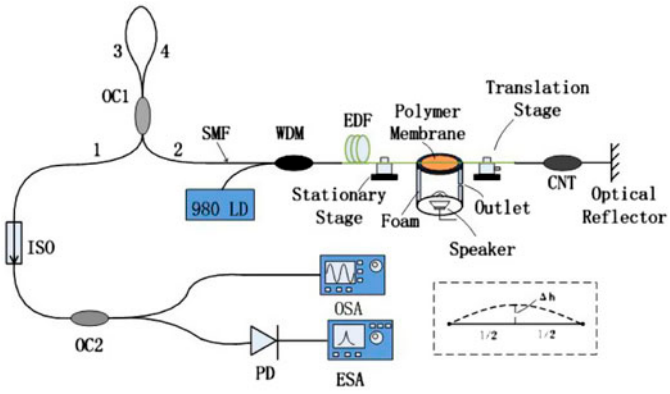

Figure 1. Schematic diagram of passively mode-locked multi-longitudinal mode FLS. OC: optic fiber coupler; ISO: isolator; CNT: carbon nanotubes; PD: photodetector; OSA: optical spectrum analyzer; ESA: electron spectrum analyzer. (The colour version of this figure is included in the online version of the journal.)

lasing and the CNT to use as a saturable absorber (SA). When the pump laser is sufficiently robust, many longitudinal modes with the same fundamental frequency spacing, $v_0 = c/2nL$, can be established in the laser cavity, where L is the cavity length, n is the effective refractive index, and c is the light velocity in vacuum.

Under an appropriate pump power at 980 nm, the proposed multi-longitudinal mode fiber laser would operate in steady state. The beat frequency between any two longitudinal modes v_p and v_q ($q < p$, $p - q = N$) can be generated on the photodetector (PD) as $f_N = v_p - v_q = (p-q)c/2nL = Nc/2nL = Nv_0$. As is known, a linear relationship between beat frequency shift and strain applied on the cavity can be expressed as [11]:

$$\Delta f_N = -N\frac{c}{2nL}\left(\frac{\delta n}{n} + \frac{\delta L}{L}\right) = -0.78 f_N \varepsilon, \qquad (1)$$

where ε means the applied strain. Equation (1) shows that the strain can be monitored by measuring the beat frequency between any two modes, The axial strain in the cavity is induced by the deformation of the membrane in a cylindrical box, as shown in Figure 1. Since the deformation of the round polymer membrane would be caused by acoustic pressure, the deformation Δh can be expressed as [7]:

$$\Delta h = \frac{3P(1-\mu^2)r^4}{16Ed^3}, \qquad (2)$$

where P represents the generated acoustic pressure, μ and E are the polymer membrane's Poisson's ratio and Young's modulus, respectively, r is the radius, and d is the thickness of the membrane. As depicted in the dashed box in Figure 1, one can simply regard the dashed curve as inclined lines for weak deformation of the membrane; hence we obtain the relative length change, i.e. axial strain, as:

$$\varepsilon = \frac{\Delta l}{l} = \frac{2\sqrt{l^2/4 + \Delta h^2} - l}{l} = 2\sqrt{1/4 + (\Delta h/l)^2} - 1, \qquad (3)$$

where l is the length of the applied strain between the stationary stage and the translation stage. Substituting Equation (2) into Equation (3), and then into Equation (1), we obtain the relationship between beat frequency shift and acoustic pressure disturbance as:

$$\Delta f_N = -0.78 f_N \left\{\sqrt{1 + \left[\frac{3P(1-\mu^2)r^4}{8Ed^3 l}\right]^2} - 1\right\}. \qquad (4)$$

Equation (4) indicates that the beat frequency will decrease when acoustic pressure increases.

3. Experiment and results

With a robust pump power pumping at 980 nm from the wavelength division multiplexing (Figure 1), the isolator (ISO) allows the signal light to propagate in only one direction. The interrogation system consists of an optical spectrum analyzer (OSA), a photodetector (PD), and an electron spectrum analyzer (ESA). The optical spectrum of the multi-longitudinal mode laser can be stably established, as displayed in Figure 2(*a*), with a broadband spectral of 3 dB and a wavelength bandwidth of about 8 nm, comparable with that reported in [10]. The corresponding frequency spectrum is given by Figure 2(*b*); it is apparent that the fundamental frequency spacing is approximately 10 MHz, which implies a cavity length about 10 m. That is basically consistent with the actual situation.

Notice from Equation (4) that the beat frequency shift is proportional to the frequency of the beat sensing signal (BSS), and thus a low-frequency BSS has relatively poor sensitivity. However, a higher frequency BSS will gradually become weak in intensity. Therefore, a

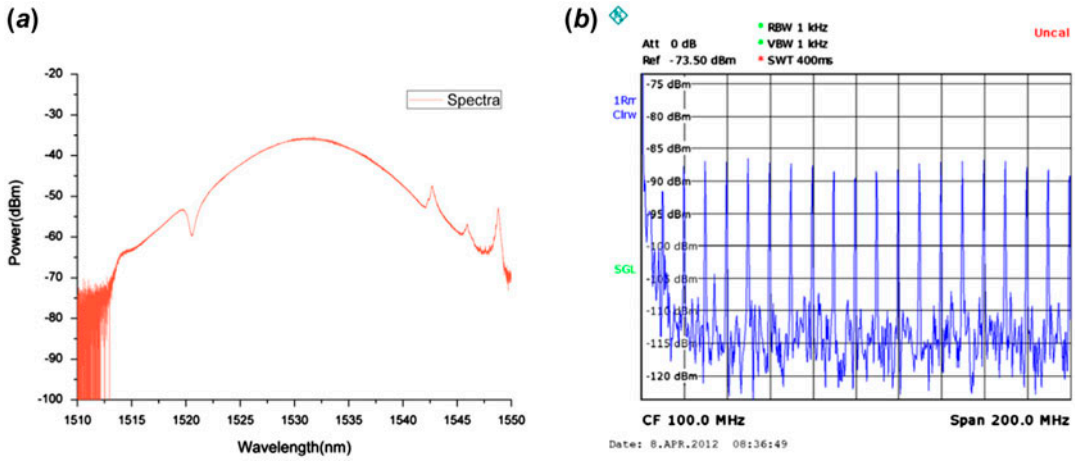

Figure 2. Optical spectrum (a) and the corresponding frequency spectrum of the multi-longitudinal mode laser sensor (b). (The colour version of this figure is included in the online version of the journal.)

trade-off is needed to ensure the BSS has both relatively high sensitivity and a strong signal-to-noise ratio (SNR). Here, a beat frequency of 5937 MHz is chosen for measurement, as shown in Figure 3, which shows that the SNR is around 20 dB with a 3 dB linewidth at about 1 kHz. In addition, demodulation of the signal in the frequency domain is easy and reliable compared with phase demodulation in the optical domain.

Before measurement of the acoustic pressure, a strain test was implemented to examine the performance of the FLS used in the current paper. Using the setup depicted in Figure 1, the stationary stage was fixed and then the translation stage moved by a step of 50 μm. The distance

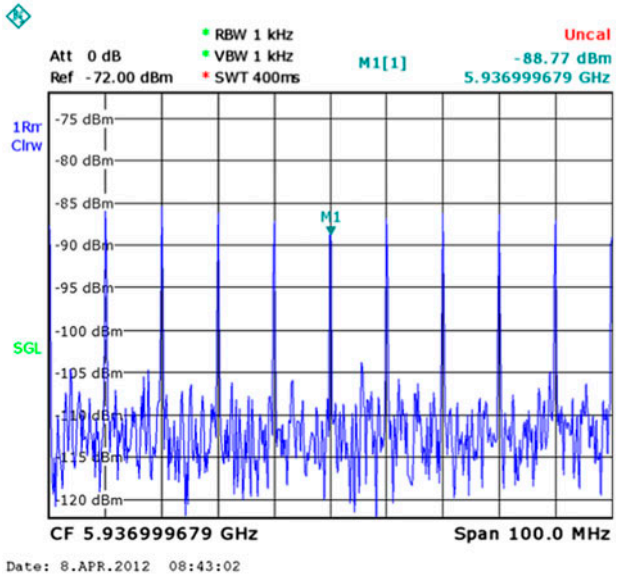

Figure 3. The chosen BSS of the proposed FLS with SNR about 20 dB. (The colour version of this figure is included in the online version of the journal.)

between the stationary stage and translation stage is 1.125 m. Results of the strain test are shown in Figure 4. From Figure 4(*a*), it can be seen that the BSS will shift to a lower frequency as the strain increases. The corresponding strain sensitivity is −535.4 Hz/$\mu\varepsilon$ with a linear regression value R^2 = 0.998, as shown in Figure 4(*b*). These values are comparable with those reported in [11]. The almost equal sensitivity in the opposite direction with good linearity is also presented, which manifests good reproducibility.

Experimental investigations for acoustic pressure measurement were carried out with a suitable pre-strain applied on the EDF between the stationary stage and the translation stage, as shown in Figure 1. A cylindrical box with a small outlet is employed to simulate an instantaneous sound pressure environment and weaken the influence of the external acoustic pressure disturbance. At the top of the box, a round polymer membrane with low Young's modulus is clamped around, operating as a transducer. It is worth mentioning that a piece of foam is used tightly close to the inner wall of the cylinder to imitate a small anechoic sound chamber. A small outlet in the box can maintain balance between inside atmospheric pressure and outside one to ensure the accuracy of measurement.

Acoustic pressure measurement results are shown in Figure 5. Obviously, with the acoustic pressure increasing, the BBS shifts to low frequency, which is in good agreement with Equation (4). In addition, apparent waveform distortion can be seen when sound pressure is increased to comparable high ones (~20 Pa). As is known, the human ear can withstand, or common speakers can produce, a maximum sound pressure of about 20 Pa [13]. Therefore, when the speaker works at overload, the sound began to distort. On the other hand, when the sound pressure is large, the sensor head and speaker obviously vibrate; this

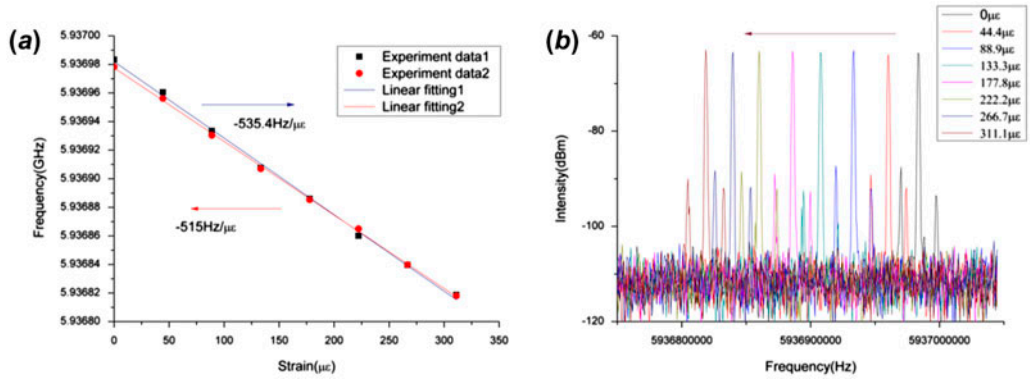

Figure 4. The strain test of the proposed FLS with sensitivity ~0.5 kHz/$\mu\varepsilon$ and good linearity. (The colour version of this figure is included in the online version of the journal.)

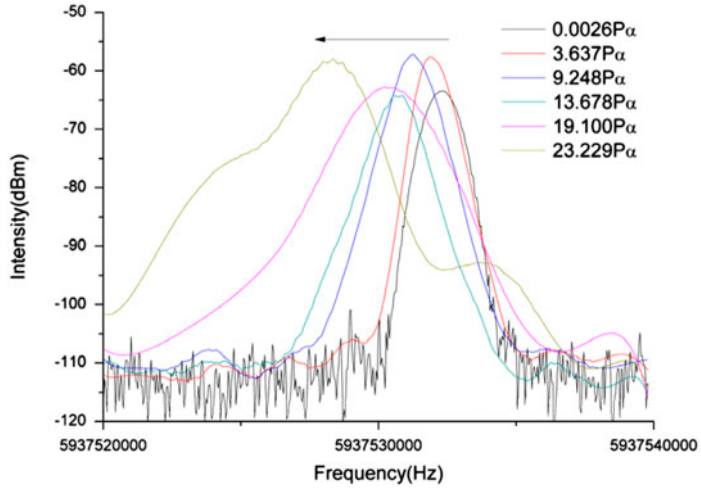

Figure 5. Acoustic pressure measurement result of the FLS sensor in a sound pressure range of 0–23 Pa. (The colour version of this figure is included in the online version of the journal.)

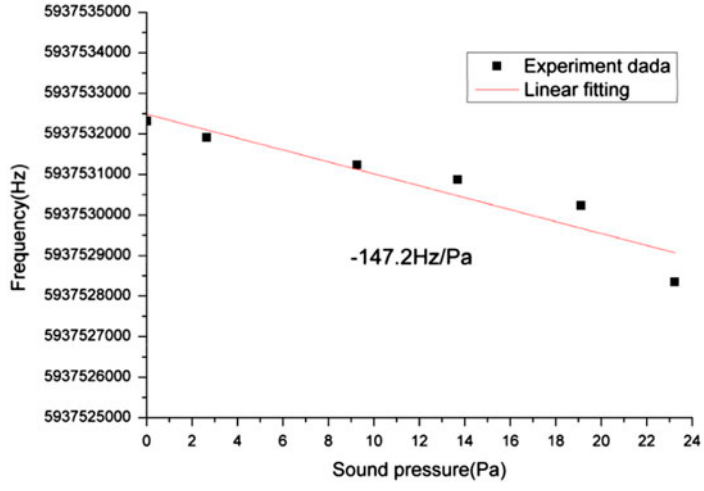

Figure 6. The frequency response against sound pressure. (The colour version of this figure is included in the online version of the journal.)

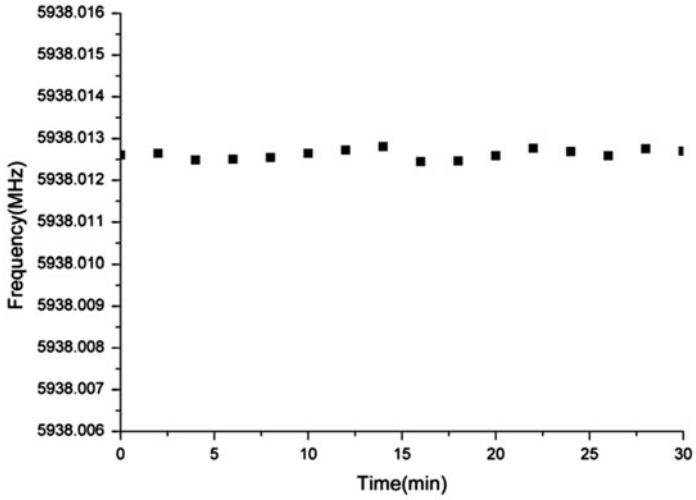

Figure 7. The frequency fluctuation around 5938.01 MHz within 30 minutes.

will also lead to spectral distortion. Thus, the range of sound pressure is greatly limited by our speaker.

The measured frequency response against sound pressure is shown in Figure 6, which shows that the frequency-to-sound pressure sensitivity –147.2 Hz/Pa in the range 0–23 Pa. It should be noted that the sound pressure range is limited by the common speaker used in our experiment and the proposed sensor has the potential to be used over a wider sound pressure range. Data sets show a relatively good linearity.

The repeatability of the corresponding sensor acoustic pressure has been measured, and the pressure measurement is repeatable for the same sensor. In order to test the stability of the proposed sensor, experimental results were recorded over some time. Figure 7 shows that the frequency stability was around 5938.01 MHz over 30 min. The fluctuation was around ±0.18 kHz. Considering that temperature has a similar influence on the fiber, the sensor can also be regarded as a temperature sensor. By comparing the thermo-optical coefficient and thermal expansion coefficient of silica fiber [14], the fluctuation is about ±0.003 K which is relatively very stable. In the sensor, the BSS is stable owing to the employment of CNT to reduce the impact of mode hopping and polarization hole burning.

4. Conclusions

In conclusion, we have demonstrated a multi-longitudinal mode fiber laser acoustic pressure sensor based on passive mode locking which employs CNT in the laser DBR cavity. This approach offers an alternative way to detect acoustic pressure and it exhibits advantages of good stability, low cost, and simpler frequency domain demodulation than conventional interferometric scheme by measuring the beat frequency using an ESA. The dimensions of the proposed sensor may be one possible disadvantage, because the laser cavity is several meters long. The sensor's sensitivity and performance can be improved by optimizing the sensor element design. For example, if the fiber is coated with a material of low bulk modulus, just like the polymer membrane used in our experiment, the strains in the fiber are significantly altered. Since plastic-coated optical fiber exhibits an order of magnitude increase in pressure sensitivity [15], this approach has been widely used in fiber optic hydrophones. That related test is a work in progress.

Funding

This work is supported by the Natural Science Foundation of China [grant number 60937002], [grant number 61275083].

References

[1] Tan, Y.; Zhang, Y.; Guan, B. *IEEE Sens. J.* **2011,** *11*, 1169–1172.
[2] Tsuda, H.; Kumakura, K.; Ogihara, S. *Sensors* **2010,** *10*, 11248–11258.
[3] Wu, Q.; Okabe, Y. *Opt. Express* **2012,** *20*, 28353–28362.
[4] Azmi, A.; Sen, D.; Sheng, W.; Canning, J.; Peng, G. *J. Lightwave Technol.* **2011,** *29*, 3453–3460.
[5] Wang, W.; Wu, N.; Tian, Y.; Wang, X.; Niezrecki, C.; Chen, J. *Opt. Express* **2009,** *17*, 16613–16618.
[6] Akkaya, O.; Kilic, O.; Digonnet, M.; Kino, G.: Solgaard, O. In *High-Sensitivity Thermally Stable Acoustic Fiber Sensor*, Proceedings of the IEEE Sensors Conference, Waikoloa, HI, Nov 01–04, 2010; pp 1148–1151.
[7] Chen, L.; Chan, C.; Yuan, W.; Goh, S.; Sun, J. *Sens. Actuators, A* **2010,** *163*, 42–47.
[8] Ma, L.; Hu, Y.; Luo, H.; Hu, Z. *IEEE Photonics Technol. Lett.* **2009,** *21*, 1280–1282.
[9] Liu, S.; Yin, Z.; Zhang, L.; Gao, L.; Chen, X.; Cheng, J. *Opt. Lett.* **2010,** *35*, 835–837.

[10] Set, S.; Yaguchi, H.; Tanaka, Y.; Jablonski, M. Presented at the Optical Fiber Communications Conference, Atlanta, GA, March 25–28, 2003.
[11] Liu, S.; Gao, L.; Yin, Z.; Zhang, L.; Chen, X.; Cheng, J. *Proc. SPIE* **2011,** *7990*, 799003.
[12] Løvseth, S; Kringlebotn, J.; Rønnekleiv, E.; Bløtekjær, K. *Appl. Opt.* **1999,** *38*, 4821–4830.
[13] Anthonyhcole, "Differentiate threshold of hearing and threshold pain", Wiki Answers, **2011**.
[14] Hadeler, O.; Rønnekleiv, E.; Ibsen, M.; Laming, R. *Appl. Opt.* **1999,** *38*, 1953–1958.
[15] Kringlebotn, J.; Archambault, J.; Reekie, L.; Payne, D. *Opt. Lett.* **1994,** *19*, 2101–2103.